Causal links between sea-ice variability in the Barents-Kara Seas and oceanic and atmospheric drivers

Jakob Dörr [1], Marius Årthun [1], David Docquier [2], Camille Li [1]and Tor Eldevik [1]

[1]Geophysical Institute, University of Bergen and Bjerknes Centre for Climate Research, Bergen, Norway
[2]Royal Meteorological Institute of Belgium, Brussels, Belgium

Key Points:

- Ocean heat transport drives sea-ice variability in the central and northeastern Barents Sea
- Atmospheric temperature drives sea-ice variability in the northern Barents-Kara Seas
- Atmospheric circulation over the Nordic Seas drives ocean heat transport, which then influences sea-ice variability

Corresponding author: Jakob Dörr, jakob.dorr@uib.no

Abstract

The sea-ice cover in the Barents and Kara Seas (BKS) displays pronounced interannual variability. Both atmospheric and oceanic drivers have been found to influence sea-ice variability, but their relative strength and regional importance remain under debate. Here, we use the Liang-Kleeman information flow method to quantify the causal influence of oceanic and atmospheric drivers on the annual sea-ice cover in the BKS in the Community Earth System Model large ensemble and reanalysis. We find that atmospheric drivers dominate in the northern part, ocean heat transport dominates in the central and northeastern part, and local sea-surface temperature dominates in the southern part. Furthermore, the large-scale atmospheric circulation over the Nordic Seas drives ocean heat transport into the Barents Sea, which then influences sea ice. Under future sea-ice retreat, the atmospheric drivers are expected to become more important.

Plain Language Summary

The sea ice in the Barents and Kara Seas is melting due to Arctic warming, but this is overlaid by large natural variability. This variability is caused by variations in the ocean and the atmosphere, but it is not clear which is more important in which parts of the region. We use a relatively new method that allows us to quantify cause-effect relationships between sea ice and atmospheric and oceanic drivers. We find that in the north of the Barents and Kara Seas, the atmosphere has the biggest impact, in the central and northeastern parts, it is the heat from the ocean, and in the south, it is the local sea temperature. We also find that wind patterns over the Nordic Seas affect how much oceanic heat comes into the Barents Sea, and that, in turn, affects the sea ice. Looking ahead, as the ice is expected to melt more in the future, the atmosphere is likely to become more important in driving sea ice variability in the Barents and Kara Seas. This study helps us better understand how the ocean and atmosphere work together to influence the yearly changes in sea ice in this region.

1 Introduction

Arctic sea ice has been retreating in all seasons since the late 1970s, mainly as a result of anthropogenic greenhouse gas emissions and associated global warming (Notz & Stroeve, 2016). In winter, sea ice in the Arctic is currently retreating fastest in the Barents and Kara Seas (BKS), which are already almost ice-free in summer (Onarheim

et al., 2018) and will continue to lose their winter sea-ice cover unless emissions are strongly reduced (Årthun et al., 2021). However, the externally forced retreat of sea ice in the BKS is overlaid by substantial internal variability on interannual to decadal timescales, which may have contributed substantially to the recent decline in the region (Onarheim & Årthun, 2017; England et al., 2019; Dörr et al., 2023). Internal variability is the dominant source of uncertainty in sea-ice projections in the Barents Sea over the next 30 years (Bonan et al., 2021), and it is therefore important to understand the underlying drivers.

Oceanic and atmospheric processes both drive sea-ice variability in the BKS, but their relative contributions remain under debate. Variable ocean heat transport toward the Arctic, mainly through the Barents Sea Opening (Figure 1) and to a lesser extent through Fram Strait, has been found to influence sea-ice variability in the BKS on seasonal to decadal timescales (Årthun et al., 2012; Sandø et al., 2014; Nakanowatari et al., 2014; Yeager et al., 2015; Årthun et al., 2019; Dörr et al., 2021; Lien et al., 2017; Docquier & Königk, 2021; Oldenburg et al., 2023). On the other hand, studies also find that atmospheric variability dominates interannual sea-ice variability in the BKS through the advection of warm air and enhancement of downward long-wave radiative fluxes, and that ocean heat transport plays a smaller role on interannual timescales (Sorokina et al., 2016; Woods & Caballero, 2016; Kim et al., 2019; Olonscheck et al., 2019; Liu et al., 2022; Zheng et al., 2022).

Common to most studies about oceanic or atmospheric drivers of sea-ice variability is the use of (lagged) anomaly correlations to infer causal mechanisms. Correlation in itself, however, does not imply causality. To identify cause and effect, causal inference frameworks can be used (examples of climate applications include Deza et al. (2015); Kretschmer et al. (2016); Vannitsem and Ekelmans (2018); Rehder et al. (2020)). One such framework, the Liang-Kleeman information flow (Liang & Kleeman, 2005; Liang, 2021), is particularly interesting because it can quantify the direction and magnitude of causal relationships. It has been used to determine causal drivers of variability in global mean temperature (Stips et al., 2016), Antarctic ice sheet surface mass balance (Vannitsem et al., 2019), and pan-Arctic sea-ice area (Docquier et al., 2022). Docquier et al. (2022) identified air temperature, sea surface temperature, and ocean heat transport as important drivers of sea ice variability, but did not consider the spatially non-uniform character of sea ice changes and their drivers, potentially mixing signals from different regions in the Arctic. Considering spatial differences in the drivers of sea-ice variability

is especially important in the BKS because of the large changes in the last decades which may lead to changes in the importance of atmospheric and oceanic drivers.

In this work, we apply the Liang-Kleeman information flow method to data from a large ensemble of climate model simulations and reanalysis products, allowing us to determine the past and future relationships between interannual variability in BKS sea-ice cover and its potential oceanic and atmospheric drivers. In section 2, we describe the data and methodology, in section 3, we present our results, and we then discuss our results and conclude in section 4.

2 Materials and Methods

We focus our analysis on output from the Community Earth System Model 1 Large Ensemble (CESM-LE; Kay et al. (2015)). CESM-LE has been widely used to assess Arctic sea-ice changes and is one of the best-performing large ensembles in reproducing the patterns and amplitude of sea-ice variability (England et al., 2019; Årthun et al., 2019). CESM-LE consists of 40 members, of which we analyze output from 1920–2079, simulated using the historical scenario before 2005 and the high emission scenario RCP8.5 (Riahi et al., 2011) after 2005. To assess changes in causal relationships, we split the period into two 80-year sub-periods (1920–1999 and 2000–2079). The large number of ensemble members ensures a robust analysis of causal drivers. Before the analysis, we remove the ensemble mean (i.e., the forced signal) from each member, such that we only analyze internal variability. Additionally, we analyze causal relationships in reanalysis data from 1979 – 2021, using ERA5 atmospheric reanalysis (Hersbach et al. (2020); 850hPa air temperature, 300hPa geopotential height, sea-level pressure) and ORAS5 ocean reanalysis (Zuo et al. (2019); sea-ice concentration, ocean velocity and temperature, sea-surface temperature). ORAS5 shows skill in reproducing observed variability and trends in temperatures in the BKS (Li et al., 2022; Shu et al., 2021; Polyakov et al., 2023). We note that the results based on this relatively short single realization will be less robust than those from CESM-LE. To remove the forced signal in reanalysis data, we detrend the data using a linear fit. The forced response is likely not linear over time, and removing a linear fit is thus not the perfect way of isolating internal variability. Nevertheless, our results remain similar if we instead remove a second-order polynomial fit (not shown).

To represent the sea-ice cover in the BKS, we calculate the sea-ice area (SIA) in the region, multiplying the sea-ice concentration with the grid cell area and summing up over all grid cells in the region (Fig. 1a). The drivers analyzed herein were chosen based on the literature on the atmospheric and oceanic influences on Arctic and BKS sea ice: ocean heat transport through the Barents Sea Opening (BSO; Årthun et al. (2012)) and the northward ocean heat transport in the Fram Strait (Fig. 1b), sea-surface temperature over the southwestern Barents Sea (SST_{AW}, Fig. 1c, Sandø et al. (2014)), air temperature at 850 hPa (T850, Fig. 1d, Olonscheck et al. (2019); Liu et al. (2022), Schlichtholz (2011)), the 300 hPa geopotential height over the extended BKS (Fig. 1e, Liu et al. (2022)), and the sea-level pressure over the northern Nordic Seas (Fig. 1f; Dörr et al. (2021); Rieke et al. (2023)). We compute the ocean heat transport on the original grids of CESM and ORAS5 through the sections shown in Fig. 1, using a reference temperature of 0°C, following Dörr et al. (2021). We compute annual means for all variables, to focus on interannual variability. CESM-LE shows trends similar to the reanalysis in all variables (Fig. 1), but simulates a lower sea-surface temperature and ocean heat transport, and more sea ice.

We use the atmospheric temperature above the boundary layer (T850) since it is less directly tied to sea ice than surface temperatures (Pavelsky et al., 2011; Olonscheck et al., 2019), and, hence, better captures the dynamical link between atmospheric variability and variability in sea ice. The influence of atmospheric temperature on sea ice occurs mostly through changes in the surface turbulent heat (latent and sensible) and long-wave radiative fluxes (Sorokina et al., 2016; Liu et al., 2022; Kim et al., 2019; Woods & Caballero, 2016). Since our analysis is based on annual means and spatial averages over areas with seasonal ice cover, it will integrate flux anomalies that both drive and are driven by sea-ice anomalies. We, therefore, do not include surface fluxes as a potential driver of sea-ice variability. Thermodynamic forcing through anomalous downwelling longwave radiative flux at the surface, which is suggested to be a main atmospheric driver of sea ice variability, is related to anticyclonic anomalies over the eastern BKS (Liu et al., 2022) and is captured by the geopotential height index.

To reveal the causal relationships between BKS sea ice and its potential drivers, we use the Liang-Kleeman information flow method (Liang & Kleeman, 2005; Liang, 2021). The method computes the absolute rate of information transfer from variable X_j to vari-

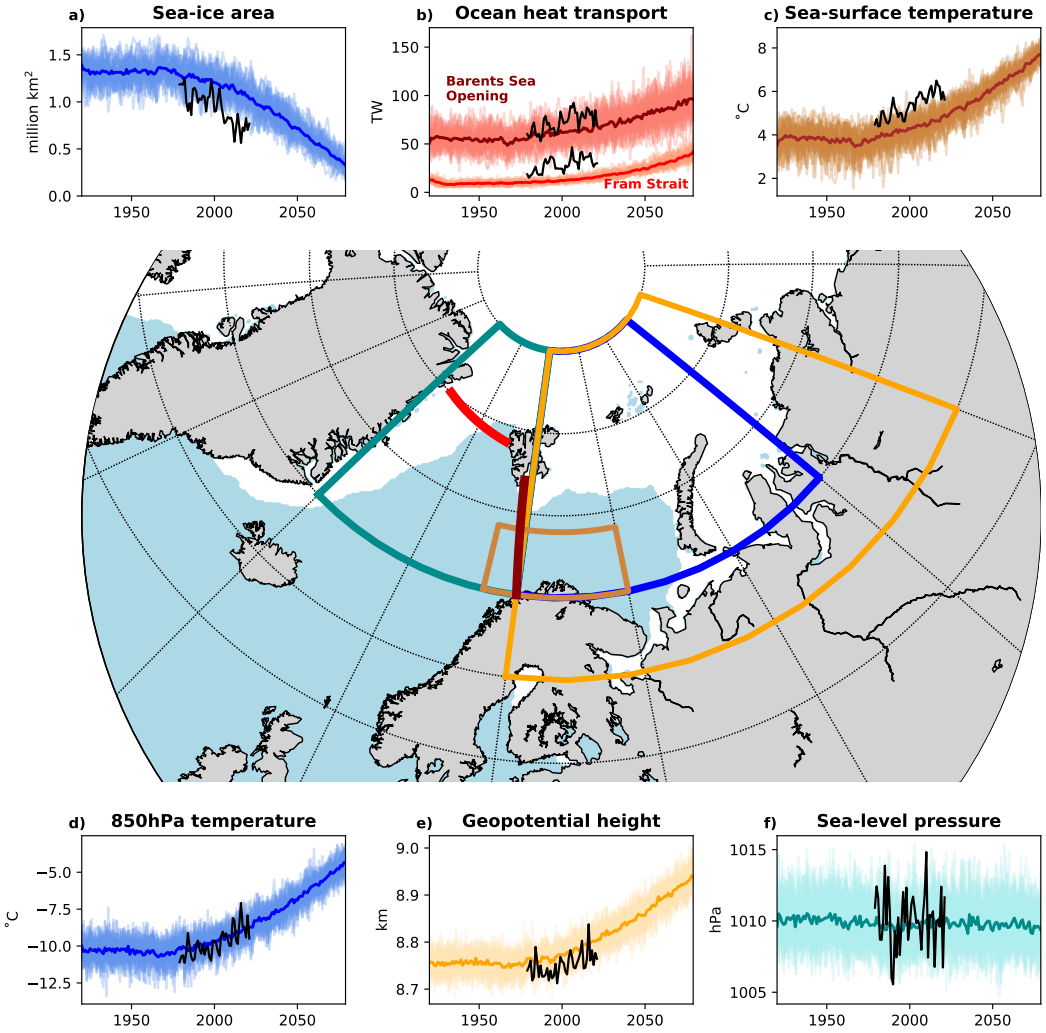

Figure 1. Potential drivers of sea-ice variability Barents-Kara Seas. a) Sea-ice area averaged over the Barents-Kara Seas (blue area; 20–80°E, 70–85°N), b) ocean heat transport through the Fram Strait (red line) and Barents Sea Opening (dark red line), c) sea-surface temperature averaged over the southwestern Barents Sea (brown area; 15–40°E, 70–74°N), d) 850 hPa temperature averaged over the BKS, e) 300 hPa geopotential height averaged over the extended BKS (orange area; 20–100°E, 65–85°N), and f) sea-level pressure averaged over the Nordic Seas (dark cyan area; -20–20°E, 70–85°N). Colored lines and shading show the ensemble mean and all individual members, respectively. Black lines show data from ERA5/ORAS5 reanalysis. White/blue shading on the map shows the annual mean sea-ice cover (based on 15% sea-ice concentration) in ORAS5 over 1979–2021.

able X_i as

$$T_{j\to i} = \frac{1}{\det\mathbf{C}} \cdot \sum_{k=1}^{N} \Delta_{jk} C_{k,dj} \cdot \frac{C_{ij}}{C_{ii}} \tag{1}$$

where $\mathbf{C}$ is the covariance matrix, N is the number of variables (7 in our case; SIA and 6 potential drivers), Δ_{jk} are the cofactors of $\mathbf{C}$, $C_{k,dj}$ is the sample covariance between X_k and the Euler forward difference in time of X_j, C_{ij} is the sample covariance between X_i and X_j and C_{ii} is the sample variance of X_i. When X_j has a causal influence on X_i, $T_{j\to i}$ is significantly different from zero, whereas when there is no influence, $T_{j\to i}$ is zero. We compute statistical significance using bootstrap resampling with replacement of all terms in Eq. (1) using 1000 realizations. We further normalize the rate of information transfer and express it in percent, as the absolute value of the relative rate of information transfer $|\tau_{j\to i}|$ (see Liang (2021) for more details). A value of $|\tau_{j\to i}|$ of 100% means a maximum influence, while 0% means no influence. Note that the percentage cannot be quantitatively interpreted as an explained variance, however, values can be compared to determine which variables have the largest influence.

We apply the Liang-Kleeman information flow method to the BKS sea ice area and the six potential drivers mentioned above. For CESM-LE, we follow Docquier et al. (2022) and compute $|\tau|$ for each member's detrended data (ensemble mean removed) and then compute the mean across ensemble members. Statistical significance is calculated using Fisher's method for multiple tests (Fisher, 1992). Furthermore, to analyze spatial differences in the causal relationships between BKS sea ice and its drivers, we repeat the analysis for each grid point in the BKS and replace the total SIA with the annual mean sea-ice concentration at this grid point. We then obtain spatial maps of the relative rate of information transfer between local sea-ice concentration and the same regional drivers mentioned above. We calculate significance for each grid point in the same way as for the sea-ice area, but we additionally apply a False Discovery Rate (FDR; Wilks (2016); Docquier et al. (2023)) to account for the multiplicity of tests.

3 Results

3.1 Causal links in CESM-LE

We first assess the causal relationships between the BKS sea-ice area and its potential drivers in CESM-LE for the two different periods, 1920–1999 and 2000–2079. Figure 2 shows matrices of the relative rates of information transfer and correlation coef-

ficients between sea ice and all its potential drivers, averaged over all CESM-LE members. In both periods, the self-influence (diagonal) shows the highest $|\tau|$, ranging from 29% to 62%. Self-influence can be interpreted as the influence of the variable state on the dynamics of the variable itself (Liang, 2021; Docquier et al., 2022).

As for the causal influence between sea ice and the other variables, the heat transport through the Barents Sea Opening has the largest influence on sea ice area in the BKS during the two periods ($|\tau|$ = 10% in 1920–1999 and 6% in 2000–2079; Fig. 2a,c), despite not being the variable with the highest correlation (R = -0.63 in 1920–1999 and -0.45 in 2000–2079; Fig. 2b,d). The second variable having a significant influence on sea ice is T850 ($|\tau|$ = 4% in 1920–1999 and 7% in 2000–2079). SST_{AW} is highly correlated to the sea-ice area (R = -0.81 in 1920–1999 and -0.69 in 2000–2079) but does not have a significant causal influence on sea ice in either period. This shows the usefulness of the causal analysis, as it identifies actual causal links rather than simple correlations between variables. Despite being significantly correlated with the sea ice area, the influence of the atmospheric circulation indices (geopotential height and sea-level pressure) on the sea ice is not significant.

Besides influencing the sea ice area, the heat transport through the Barents Sea Opening also influences SST_{AW} in both periods (fourth row in Fig. 2a,c). This underscores the importance of the oceanic heat imported into the Barents Sea in setting the ocean temperatures and ice cover (Årthun et al., 2012). Furthermore, CESM-LE shows a significant correlation between the heat transport through Fram Strait and the Barents Sea Opening in the first period (R = 0.49), which is likely due to similar atmospheric influence (Dörr et al., 2021). The information flow method picks up this connection as an influence from the Barents Sea Opening to the Fram Strait ($|\tau|$ = 10%), which is expected since the Barents Sea Opening is upstream of the Fram Strait. Finally, the variability in Barents Sea Opening heat transport is significantly influenced by sea-level pressure over the Nordic Seas during the first period ($|\tau|$ = 5%), confirming that interannual variability of ocean heat transport is driven by atmospheric circulation (Muilwijk et al., 2019; Dörr et al., 2021; Madonna & Sandø, 2022; Brown et al., 2023). These results suggest that for annual means, the direct influence of the large-scale atmospheric circulation on sea ice in the BKS is weak, but a causal chain exists whereby the Nordic sea-level pressure influences the oceanic heat transport into the BKS, which then influences sea ice.

In the second period, as the sea ice retreats northward, the influence of the Barents Sea Opening heat transport on sea ice becomes weaker ($|\tau| = 6\%$, Fig. 2c). On the other hand, the influence of T850 becomes larger ($|\tau| = 7\%$), indicating that atmospheric temperatures will be increasingly important for sea-ice variability in the future BKS. The influence of sea-level pressure over the Nordic Seas on the Barents Sea Opening heat transport weakens and is no longer significant in the second period, while their correlation stays high. We note that when we expand the area over which we average the sea-level pressure to the south, its influence is still significant in both periods (not shown), indicating that the large-scale influence of the atmospheric circulation over the Nordic Seas remains an important driver of ocean heat transport into the Barents Sea.

We next look at the spatial distribution of the causal relationships between sea ice and its potential drivers in CESM-LE by replacing the BKS sea ice area with the local sea ice concentration and repeating the analysis for every grid point in the BKS. We show the causal relationship in both directions for sea ice and the Barents Sea Opening heat transport, T850, SST_{AW}, and the geopotential height index for the second period in Figure 3. We choose to show the second period only (2000–2079) because it is the period where the average sea-ice area is closer to the reanalysis data (Fig. 1). We show the interaction of sea ice with all variables during both periods in Supplementary Figures S1 and S2.

The causal method reveals that atmospheric temperatures (T850) mainly influence sea ice in the northern and eastern BKS, while sea-surface temperatures in the southern Barents Sea (SST_{AW}) mainly influence sea ice in the central and southern Barents Sea (Fig. 3a,b left). The regions of significant influence are broadly consistent with the regions of maximum correlation (right column in Fig. 3a,b), although the correlations are significant in the entire BKS region for both variables. The local influence of the Barents Sea Opening heat transport on sea ice is significant in the northeastern Barents Sea, approximately in between the influence regions of T850 and SST_{AW} (Fig. 3c). However, unlike the correlation, which also shows a maximum in the southern BKS, $|\tau|$ is not significant there, indicating no direct influence of the Barents Sea Opening heat transport on sea ice in this region. The results show a similar tripartition in the earlier period (Supplementary Fig. S2). However, the influence of SST and T850 is more limited, and the influence of the Barents Sea Opening ocean heat transport is strong across the entire Bar-

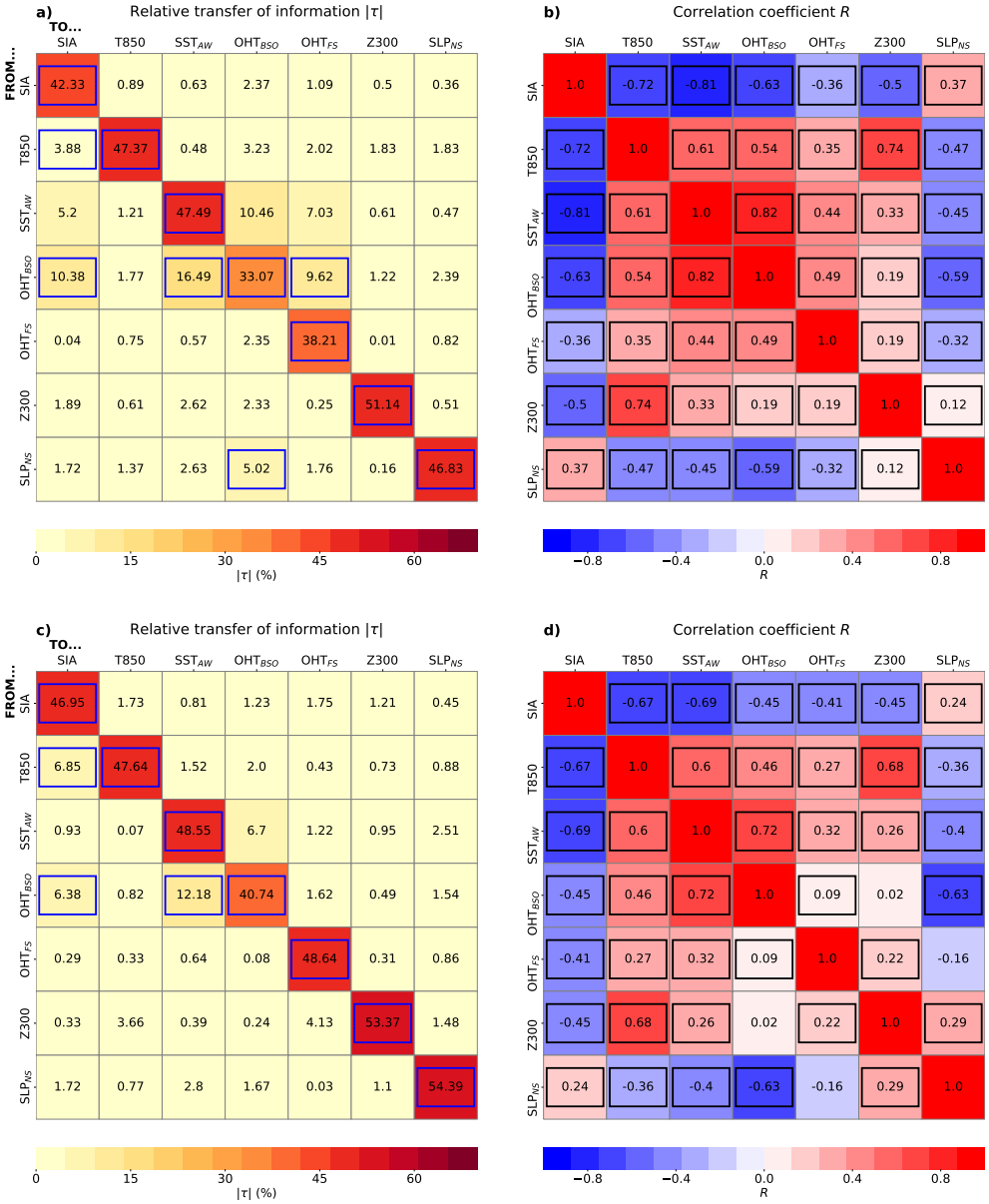

Figure 2. Causal drivers of sea ice variability in the Barents-Kara Seas (BKS). Matrix with relative rates of information transfer (a,c) and correlation coefficients (b,d) between each variable in the BKS for 1920–1999 (a,b) and 2000–2079 (c,d) averaged over 40 members from CESM-LE. Variables include the sea-ice area over the BKS (SIA), the 850 hPa air temperature (T850), the sea-surface temperature over the southwestern Barents Sea (SST_{AW}), the ocean heat transport through the Barents Sea Opening (OHT_{BSO}), the ocean heat transport through the Fram Strait (OHT_{FS}), the 300-hPa geopotential over the extended region (Z300), and the sea-level pressure over the Nordic Seas (SLP_{NS}). The highlighted elements are significant at the 5% confidence level based on Fisher's method for multiple tests.

ents Sea, which confirms results obtained with sea ice area instead of sea ice concentration (Fig. 2).

The atmospheric geopotential height index (Z300) is well correlated with the sea ice concentration in the northern BKS (as also shown in Liu et al. (2022)). The significant influence on sea ice is, however, restricted to the area south of Svalbard in the first period (Fig. S2) and almost disappears in the second period (Fig. 3e). The sea-level pressure over the Nordic Seas is well correlated to sea ice in the southern BKS, but the information flow method shows no significant influence (Fig. S1). This corroborates the result from Fig. 2 that the sea-level pressure influences sea ice in the southern Barents Sea mainly via the Barents Sea Opening heat transport.

In summary, we find that in CESM-LE, the Barents Sea Opening heat transport has the strongest influence on sea ice in the first period, mostly affecting sea ice in the central and northeastern Barents Sea. Sea ice in the northern BKS is mostly affected by atmospheric temperature, which has the strongest total influence in the second period. Sea ice in the southern Barents Sea is mostly affected by local sea-surface temperature. We further find a causal chain in which the atmosphere influences ocean heat transport into the Barents Sea, which then influences sea ice.

3.2 Causal links in reanalysis

To evaluate the results from CESM-LE, we briefly analyze causal relationships between BKS sea ice and its drivers in reanalysis data from 1979 – 2021. Because of the relatively short observational period, large internal variability, and only one realization, the relative transfer of information between the BKS sea-ice area and the other variables is not significant (Fig. S3 in the supplemental material). We therefore directly turn to the regional relationships between sea-ice concentration and T850, SST_{AW}, the Barents Sea Opening heat transport, and the geopotential height index in Figure 4. Note that we use a significance level of 10% to account for the short observational period. Even though most values are not significant, it is still useful to compare the results with those from CESM-LE. The relationship of sea ice with all variables is shown in Figure S4. Like in CESM-LE, the Barents Sea Opening heat transport significantly influences sea ice concentration in the northern and northeastern Barents Sea, although over a smaller area than in CESM-LE, and a bit more to the west. The influence of SST_{AW} is limited in re-

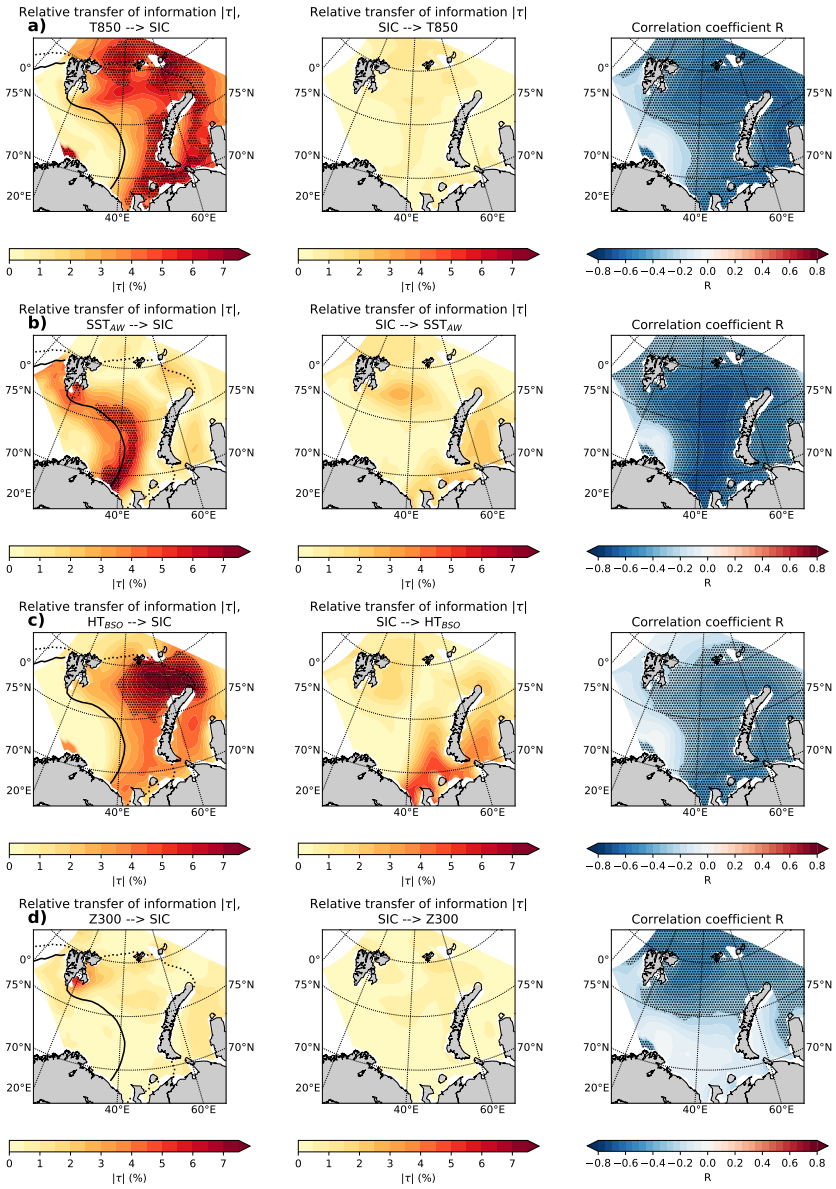

Figure 3. Regional influence on Barents-Kara Seas (BKS) sea ice. Maps of relative rates of information transfer (in the two directions) and correlation coefficients between annual mean sea-ice concentration and a) 850 hPa temperature (T850) over the BKS, b) sea-surface temperature (SST_{AW}) over the southwestern BKS, c) heat transport through the Barents Sea Opening (HT_{BSO}, and d) 300 hPa geopotential height (Z300) over the BKS, for CESM-LE over 2000–2079. The black contour line in the left panels denotes the ensemble mean sea-ice edge (based on 15% sea-ice concentration) in 2000, and the dashed line the sea-ice edge in 2079. Black stippling denotes statistically significant values (FDR 5%; 1000 bootstrap samples).

analysis. Similar to CESM-LE, the reanalysis data shows the largest (although not significant) influence of T850 in the northern BKS.

The correlation maps for sea ice and the geopotential height index (Z300) look similar to CESM-LE, with Z300 being correlated with sea-ice concentration in the northern Barents Sea (Fig. 4e). This area corresponds to elevated rates of information transfer from sea ice to Z300, albeit not significant.

Although the influences are mostly not significant, the reanalysis data generally supports the partitioning of the Barents Sea ice cover into a northern part influenced by atmospheric temperatures, and a central part influenced by ocean heat transport, although the partitioning is not as clear as in CESM-LE. Furthermore, the reanalysis also supports the notion that, for annual means and on interannual timescales, the atmospheric circulation indices have little direct influence on the sea ice cover, but instead influence the ocean heat transport into the Barents Sea (Fig. S3).

4 Discussion and Conclusions

We have used the Liang-Kleeman information flow method (Liang & Kleeman, 2005; Liang, 2021) to analyze causal relationships between annual-mean sea ice variability and its atmospheric and oceanic drivers in the Barents and Kara Seas based on the CESM-LE large ensemble (1920–2079) and reanalysis data (1979–2021). We find that in CESM-LE, the ocean heat transport into the Barents Sea is a main driver of present and future sea ice variability, consistent with previous studies (Årthun et al., 2012; Decuypère et al., 2022; Docquier et al., 2021; Dörr et al., 2021; Rieke et al., 2023). Furthermore, we find a tripartition of the Barents-Kara sea ice, with the northern part being predominantly influenced by atmospheric temperature (Arctic domain), the southern part influenced by local sea-surface temperature (Atlantic domain), and the region between the two domains influenced by ocean heat transport. We further find that as the sea ice cover in the Barents-Kara Seas retreats in the future, the influence of sea-surface temperature and ocean heat transport decreases, while the atmospheric influence increases, as suggested by Smedsrud et al. (2013).

Previous studies have identified a strong influence of atmospheric circulation patterns on subseasonal to interannual sea ice variability in the Barents and Kara Seas during the cold season, both in observations/reanalysis (Kimura & Wakatsuchi, 2001; Deser

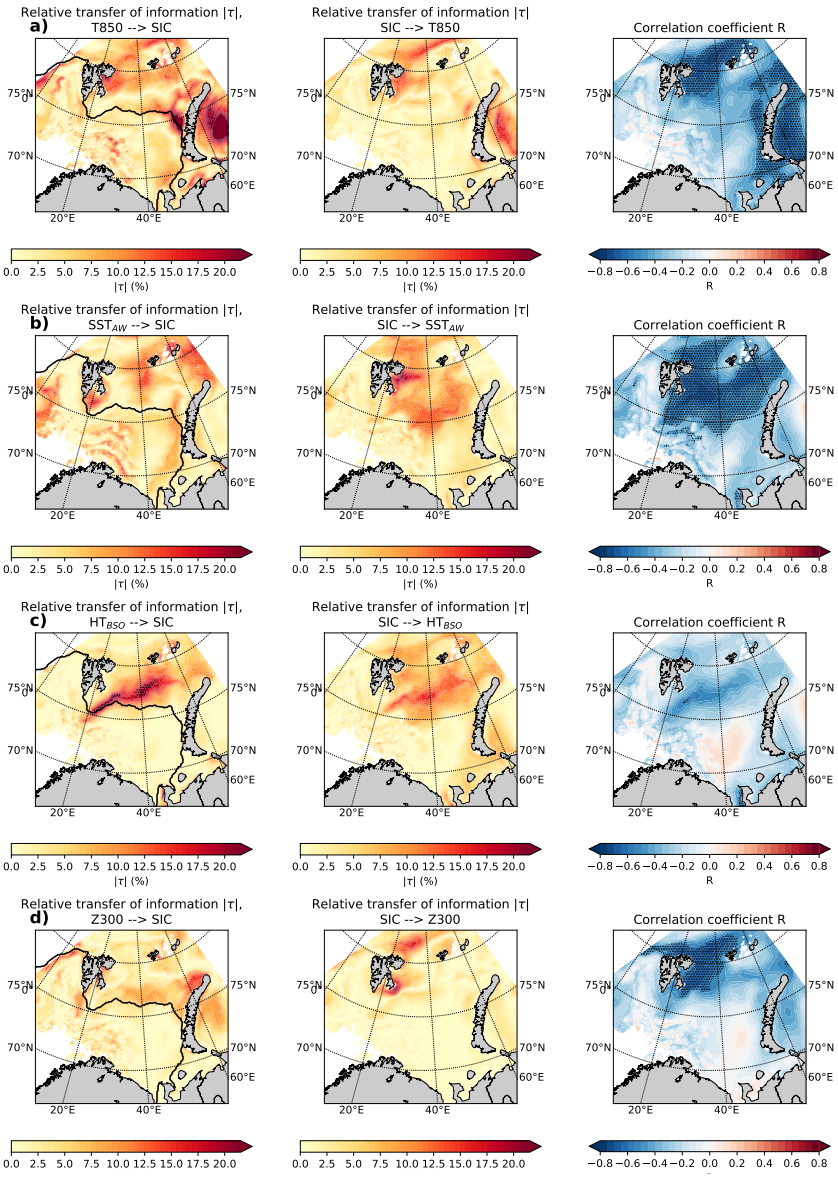

Figure 4. As Figure 3, but for ORAS5/ERA5 in 1979–2021. The black contour line in the left panels denotes the ensemble mean sea-ice edger (based on 15% sea-ice concentration) in 1979–2021. Black stippling denotes statistically significant values (FDR 10%; 1000 bootstrap samples).

et al., 2000; Sorokina et al., 2016; Blackport et al., 2019; Siew et al., 2023) and modelling experiments (Blackport et al., 2019; Liu et al., 2022; Siew et al., 2023). On decadal and longer time scales, large-scale atmospheric circulation as well as ocean heat transport and Atlantic Water properties have been found to influence sea ice variability (Zhang, 2015; Yashayaev & Seidov, 2015; Polyakov et al., 2023). Our results focusing on annual means indicate that the direct influence of circulation patterns on Barents-Kara sea ice variability is weak and regionally confined. Rather, we show indirect influences via atmospheric temperature as well as via a causal chain where the atmospheric circulation over the Nordic Seas drives variability of ocean heat transport into the Barents Sea, which then drives sea-ice variability, consistent with Sorteberg and Kvingedal (2006) and Muilwijk et al. (2019). These indirect influences seem reasonable given our use of annual-mean atmospheric circulation patterns, whose variability reflects more integrated signals of global climate change.

A main novelty of our results is that they go beyond simple correlations, which do not necessarily imply causality and do not reveal the direction of possible causal relationships. That said, the correlation is still a useful diagnostic in the case of a known relationship, such as between ocean heat transport and sea ice. Furthermore, we acknowledge the limitations of using the Liang-Kleeman information flow method. First, the method is valid for linear systems and will only give an approximate solution for non-linear systems. The method has, however, been validated using highly non-linear synthetic examples (Liang, 2021), and has been successfully used to detect causal influences in the climate system (Liang, 2014; Stips et al., 2016; Docquier et al., 2022). Non-linear estimates of the rate of information transfer (e.g., Pires et al. (2023)) have therefore not been applied here. Second, there might be hidden variables that have an influence on sea ice in the Barents-Kara Seas but that are not included here. However, we have carefully checked the literature to account for all relevant variables, so the effect of hidden variables is likely limited. Despite these two limitations, this causal method provides highly valuable information on causal drivers of annual sea ice variability in the Barents and Kara Seas beyond correlation and regression analyses.

Acknowledgments

This study was funded by the Research Council of Norway projects Nansen Legacy (grant 276730) and the Trond Mohn Foundation (grant BFS2018TMT01). David Docquier is

funded by the Belgian Science Policy Office (BELSPO) under the RESIST project (contract no. RT/23/RESIST). Camille Li is funded by the Research Council of Norway grant 325440. We thank the CESM Large Ensemble Community Project for making their data publicly accessible. The results contain modified Copernicus Climate Change Service information 2023. Neither the European Commission nor ECMWF is responsible for any use that may be made of the Copernicus information or data it contains.

Open Research

All data in this study are publicly available. Output from ORAS5 is available through the Copernicus Climate Change Service's Climate Data Store (Copernicus Climate Change Service, 2021). Output from ERA5 is available through the Copernicus Climate Change Service's Climate Data Store (Copernicus Climate Change Service, 2019a, 2019b). Output from CESM-LE is available via the Earth System Grid (Climate Data Gateway, 2021). Python functions used to calculate the Liang-Kleeman information flow as in Docquier et al. (2022) can be downloaded from `https://github.com/Climdyn/Liang_Index_climdyn`.

References

Årthun, M., Eldevik, T., & Smedsrud, L. H. (2019, March). The Role of Atlantic Heat Transport in Future Arctic Winter Sea Ice Loss. *J. Climate*, *32*(11), 3327–3341. doi: 10.1175/JCLI-D-18-0750.1

Årthun, M., Eldevik, T., Smedsrud, L. H., Skagseth, Ø., & Ingvaldsen, R. B. (2012, July). Quantifying the Influence of Atlantic Heat on Barents Sea Ice Variability and Retreat. *J. Climate*, *25*(13), 4736–4743. doi: 10.1175/JCLI-D-11-00466.1

Årthun, M., Onarheim, I. H., Dörr, J., & Eldevik, T. (2021). The Seasonal and Regional Transition to an Ice-Free Arctic. *Geophys. Res. Lett.*, *48*(1), e2020GL090825. doi: 10.1029/2020GL090825

Blackport, R., Screen, J. A., van der Wiel, K., & Bintanja, R. (2019, September). Minimal influence of reduced Arctic sea ice on coincident cold winters in mid-latitudes. *Nat. Clim. Change*, *9*(9), 697–704. doi: 10.1038/s41558-019-0551-4

Bonan, D. B., Lehner, F., & Holland, M. M. (2021). Partitioning uncertainty in projections of Arctic sea ice. *Environ. Res. Lett.*. doi: 10.1088/1748-9326/abe0ec

Brown, N. J., Mauritzen, C., Li, C., Madonna, E., Isachsen, P. E., & LaCasce,

J. H. (2023, January). Rapid Response of the Norwegian Atlantic Slope Current to Wind Forcing. *J. Phys. Oceanogr.*, *53*(2), 389–408. doi: 10.1175/JPO-D-22-0014.1

Climate Data Gateway. (2021). *Dataset: CESM1 Large Ensemble.* [Dataset] https://www.earthsystemgrid.org/dataset/ucar.cgd.ccsm4.cesmLE.html.

Copernicus Climate Change Service. (2019a). *ERA5 monthly averaged data on pressure levels from 1979 to present.* ECMWF. doi: 10.24381/CDS.6860A573

Copernicus Climate Change Service. (2019b). *ERA5 monthly averaged data on single levels from 1979 to present.* ECMWF. doi: 10.24381/CDS.F17050D7

Copernicus Climate Change Service. (2021). *ORAS5 global ocean reanalysis monthly data from 1958 to present.* ECMWF. doi: 10.24381/CDS.67E8EEB7

Decuypère, M., Tremblay, L. B., & Dufour, C. O. (2022). Impact of Ocean Heat Transport on Arctic Sea Ice Variability in the GFDL CM2-O Model Suite. *J. Geophys. Res. Oceans*, *127*(3), e2021JC017762. doi: 10.1029/2021JC017762

Deser, C., Walsh, J. E., & Timlin, M. S. (2000, February). Arctic Sea Ice Variability in the Context of Recent Atmospheric Circulation Trends. *J. Climate*, *13*(3), 617–633. doi: 10.1175/1520-0442(2000)013⟨0617:ASIVIT⟩2.0.CO;2

Deza, J. I., Barreiro, M., & Masoller, C. (2015, March). Assessing the direction of climate interactions by means of complex networks and information theoretic tools. *Chaos*, *25*(3), 033105. doi: 10.1063/1.4914101

Docquier, D., Koenigk, T., Fuentes-Franco, R., Karami, M. P., & Ruprich-Robert, Y. (2021, March). Impact of ocean heat transport on the Arctic sea-ice decline: A model study with EC-Earth3. *Clim Dyn*, *56*(5), 1407–1432. doi: 10.1007/s00382-020-05540-8

Docquier, D., & Königk, T. (2021). A review of interactions between ocean heat transport and Arctic sea ice. *Environ. Res. Lett.*. doi: 10.1088/1748-9326/ac30be

Docquier, D., Vannitsem, S., & Bellucci, A. (2023, May). The rate of information transfer as a measure of ocean–atmosphere interactions. *Earth Syst. Dyn.*, *14*(3), 577–591. doi: 10.5194/esd-14-577-2023

Docquier, D., Vannitsem, S., Ragone, F., Wyser, K., & Liang, X. S. (2022). Causal Links Between Arctic Sea Ice and Its Potential Drivers Based on the Rate of Information Transfer. *Geophys. Res. Lett.*, *49*(9), e2021GL095892. doi:

10.1029/2021GL095892

Dörr, J. S., Årthun, M., Eldevik, T., & Madonna, E. (2021, November). Mechanisms of Regional Winter Sea-Ice Variability in a Warming Arctic. *J. Climate*, *34*(21), 8635–8653. doi: 10.1175/JCLI-D-21-0149.1

Dörr, J. S., Bonan, D. B., Årthun, M., Svendsen, L., & Wills, R. C. J. (2023, February). Forced and internal components of observed Arctic sea-ice changes. *Cryosphere Discuss.*, 1–27. doi: 10.5194/tc-2023-29

England, M., Jahn, A., & Polvani, L. (2019, July). Nonuniform Contribution of Internal Variability to Recent Arctic Sea Ice Loss. *J. Climate*, *32*(13), 4039–4053. doi: 10.1175/JCLI-D-18-0864.1

Fisher, R. A. (1992). Statistical Methods for Research Workers. In S. Kotz & N. L. Johnson (Eds.), *Breakthroughs in Statistics: Methodology and Distribution* (pp. 66–70). New York, NY: Springer. doi: 10.1007/978-1-4612-4380-9_6

Hersbach, H., Bell, B., Berrisford, P., Hirahara, S., Horányi, A., Muñoz-Sabater, J., ... Thépaut, J.-N. (2020). The ERA5 global reanalysis. *Q. J. Roy. Meteor. Soc.*, *146*(730), 1999–2049. doi: 10.1002/qj.3803

Kay, J. E., Deser, C., Phillips, A., Mai, A., Hannay, C., Strand, G., ... Vertenstein, M. (2015, November). The Community Earth System Model (CESM) Large Ensemble Project: A Community Resource for Studying Climate Change in the Presence of Internal Climate Variability. *B. Am. Meteorol. Soc.*, *96*(8), 1333–1349. doi: 10.1175/BAMS-D-13-00255.1

Kim, K.-Y., Kim, J.-Y., Kim, J., Yeo, S., Na, H., Hamlington, B. D., & Leben, R. R. (2019, February). Vertical Feedback Mechanism of Winter Arctic Amplification and Sea Ice Loss. *Sci. Rep.*, *9*(1), 1184. doi: 10.1038/s41598-018-38109-x

Kimura, N., & Wakatsuchi, M. (2001). Mechanisms for the variation of sea ice extent in the northern hemisphere. *J. Geophys. Res. Oceans*, *106*(C12), 31319–31331. doi: 10.1029/2000JC000739

Kretschmer, M., Coumou, D., Donges, J. F., & Runge, J. (2016, June). Using Causal Effect Networks to Analyze Different Arctic Drivers of Mid-latitude Winter Circulation. *J. Clim.*, *29*(11), 4069–4081. doi: 10.1175/JCLI-D-15-0654.1

Li, Z., Ding, Q., Steele, M., & Schweiger, A. (2022, January). Recent upper Arctic Ocean warming expedited by summertime atmospheric processes. *Nat Com-*

mun, *13*(1), 362. doi: 10.1038/s41467-022-28047-8

Liang, X. S. (2014, November). Unraveling the cause-effect relation between time series. *Phys. Rev. E*, *90*(5), 052150. doi: 10.1103/PhysRevE.90.052150

Liang, X. S. (2021, June). Normalized Multivariate Time Series Causality Analysis and Causal Graph Reconstruction. *Entropy*, *23*(6), 679. doi: 10.3390/e23060679

Liang, X. S., & Kleeman, R. (2005, December). Information Transfer between Dynamical System Components. *Phys. Rev. Lett.*, *95*(24), 244101. doi: 10.1103/PhysRevLett.95.244101

Lien, V. S., Schlichtholz, P., Skagseth, Ø., & Vikebø, F. B. (2017, January). Wind-Driven Atlantic Water Flow as a Direct Mode for Reduced Barents Sea Ice Cover. *J. Climate*, *30*(2), 803–812. doi: 10.1175/JCLI-D-16-0025.1

Liu, Z., Risi, C., Codron, F., Jian, Z., Wei, Z., He, X., ... Bowen, G. J. (2022, September). Atmospheric forcing dominates winter Barents-Kara sea ice variability on interannual to decadal time scales. *Proc. Natl. Acad. Sci.*, *119*(36), e2120770119. doi: 10.1073/pnas.2120770119

Madonna, E., & Sandø, A. B. (2022). Understanding Differences in North Atlantic Poleward Ocean Heat Transport and Its Variability in Global Climate Models. *Geophys. Res. Lett.*, *49*(1), e2021GL096683. doi: 10.1029/2021GL096683

Muilwijk, M., Ilicak, M., Cornish, S. B., Danilov, S., Gelderloos, R., Gerdes, R., ... Wang, Q. (2019). Arctic Ocean Response to Greenland Sea Wind Anomalies in a Suite of Model Simulations. *J. Geophys. Res. Oceans*, *124*(8), 6286–6322. doi: 10.1029/2019JC015101

Nakanowatari, T., Sato, K., & Inoue, J. (2014, December). Predictability of the Barents Sea Ice in Early Winter: Remote Effects of Oceanic and Atmospheric Thermal Conditions from the North Atlantic. *J. Clim.*, *27*(23), 8884–8901. doi: 10.1175/JCLI-D-14-00125.1

Notz, D., & Stroeve, J. (2016, November). Observed Arctic sea-ice loss directly follows anthropogenic CO2 emission. *Science*, *354*(6313), 747–750. doi: 10.1126/science.aag2345

Oldenburg, D., Kwon, Y.-O., Frankignoul, C., Danabasoglu, G., Yeager, S., & Kim, W. M. (2023, December). The respective roles of ocean heat transport and surface heat fluxes in driving Arctic Ocean warming and sea-ice decline. *J.*

Clim., *-1*(aop). doi: 10.1175/JCLI-D-23-0399.1

Olonscheck, D., Mauritsen, T., & Notz, D. (2019, June). Arctic sea-ice variability is primarily driven by atmospheric temperature fluctuations. *Nat. Geosci.*, *12*(6), 430–434. doi: 10.1038/s41561-019-0363-1

Onarheim, I. H., & Årthun, M. (2017). Toward an ice-free Barents Sea. *Geophys. Res. Lett.*, *44*(16), 8387–8395. doi: 10.1002/2017GL074304

Onarheim, I. H., Eldevik, T., Smedsrud, L. H., & Stroeve, J. C. (2018, March). Seasonal and Regional Manifestation of Arctic Sea Ice Loss. *J. Climate*, *31*(12), 4917–4932. doi: 10.1175/JCLI-D-17-0427.1

Pavelsky, T. M., Boé, J., Hall, A., & Fetzer, E. J. (2011, March). Atmospheric inversion strength over polar oceans in winter regulated by sea ice. *Clim Dyn*, *36*(5), 945–955. doi: 10.1007/s00382-010-0756-8

Pires, C. A., Docquier, D., & Vannitsem, S. (2023, November). A general theory to estimate Information transfer in nonlinear systems. *Physica D: Nonlinear Phenomena*, 133988. doi: 10.1016/j.physd.2023.133988

Polyakov, I. V., Ingvaldsen, R. B., Pnyushkov, A. V., Bhatt, U. S., Francis, J. A., Janout, M., ... Skagseth, Ø. (2023, September). Fluctuating Atlantic inflows modulate Arctic atlantification. *Science*, *381*(6661), 972–979. doi: 10.1126/science.adh5158

Rehder, Z., Niederdrenk, A. L., Kaleschke, L., & Kutzbach, L. (2020, November). Analyzing links between simulated Laptev Sea sea ice and atmospheric conditions over adjoining landmasses using causal-effect networks. *The Cryosphere*, *14*(11), 4201–4215. doi: 10.5194/tc-14-4201-2020

Riahi, K., Rao, S., Krey, V., Cho, C., Chirkov, V., Fischer, G., ... Rafaj, P. (2011, August). RCP 8.5—A scenario of comparatively high greenhouse gas emissions. *Climatic Change*, *109*(1), 33. doi: 10.1007/s10584-011-0149-y

Rieke, O., Årthun, M., & Dörr, J. S. (2023, April). Rapid sea ice changes in the future Barents Sea. *The Cryosphere*, *17*(4), 1445–1456. doi: 10.5194/tc-17-1445-2023

Sandø, A. B., Gao, Y., & Langehaug, H. R. (2014). Poleward ocean heat transports, sea ice processes, and Arctic sea ice variability in NorESM1-M simulations. *J. Geophys. Res. Oceans*, *119*(3), 2095–2108. doi: 10.1002/2013JC009435

Schlichtholz, P. (2011). Influence of oceanic heat variability on sea ice anomalies in

the Nordic Seas. *Geophys. Res. Lett.*, *38*(5). doi: 10.1029/2010GL045894

Shu, Q., Wang, Q., Song, Z., & Qiao, F. (2021, May). The poleward enhanced Arctic Ocean cooling machine in a warming climate. *Nat Commun*, *12*(1), 2966. doi: 10.1038/s41467-021-23321-7

Siew, P. Y. F., Wu, Y., Ting, M., Zheng, C., Clancy, R., Kurtz, N. T., & Seager, R. (2023, August). Physical links from atmospheric circulation patterns to Barents-Kara sea ice variability from synoptic to seasonal timescales in the cold season. *J. Clim.*, *-1*(aop). doi: 10.1175/JCLI-D-23-0155.1

Smedsrud, L. H., Esau, I., Ingvaldsen, R. B., Eldevik, T., Haugan, P. M., Li, C., ... Sorokina, S. A. (2013). The Role of the Barents Sea in the Arctic Climate System. *Rev. Geophys.*, *51*(3), 415–449. doi: 10.1002/rog.20017

Sorokina, S. A., Li, C., Wettstein, J. J., & Kvamstø, N. G. (2016, January). Observed Atmospheric Coupling between Barents Sea Ice and the Warm-Arctic Cold-Siberian Anomaly Pattern. *J. Clim.*, *29*(2), 495–511. doi: 10.1175/JCLI-D-15-0046.1

Sorteberg, A., & Kvingedal, B. (2006, October). Atmospheric Forcing on the Barents Sea Winter Ice Extent. *J. Clim.*, *19*(19), 4772–4784. doi: 10.1175/JCLI3885.1

Stips, A., Macias, D., Coughlan, C., Garcia-Gorriz, E., & Liang, X. S. (2016, February). On the causal structure between CO2 and global temperature. *Sci Rep*, *6*(1), 21691. doi: 10.1038/srep21691

Vannitsem, S., Dalaiden, Q., & Goosse, H. (2019). Testing for Dynamical Dependence: Application to the Surface Mass Balance Over Antarctica. *Geophys. Res. Lett.*, *46*(21), 12125–12135. doi: 10.1029/2019GL084329

Vannitsem, S., & Ekelmans, P. (2018, August). Causal dependences between the coupled ocean–atmosphere dynamics over the tropical Pacific, the North Pacific and the North Atlantic. *Earth Syst. Dyn.*, *9*(3), 1063–1083. doi: 10.5194/esd-9-1063-2018

Wilks, D. S. (2016, December). "The Stippling Shows Statistically Significant Grid Points": How Research Results are Routinely Overstated and Overinterpreted, and What to Do about It. *Bull. Am. Meteorol. Soc.*, *97*(12), 2263–2273. doi: 10.1175/BAMS-D-15-00267.1

Woods, C., & Caballero, R. (2016, March). The Role of Moist Intrusions in Winter

525 Arctic Warming and Sea Ice Decline. *J. Climate*, *29*(12), 4473–4485. doi: 10
526 .1175/JCLI-D-15-0773.1
527 Yashayaev, I., & Seidov, D. (2015, March). The role of the Atlantic Water in multi-
528 decadal ocean variability in the Nordic and Barents Seas. *Progress in Oceanog-*
529 *raphy*, *132*, 68–127. doi: 10.1016/j.pocean.2014.11.009
530 Yeager, S. G., Karspeck, A. R., & Danabasoglu, G. (2015). Predicted slowdown
531 in the rate of Atlantic sea ice loss. *Geophys. Res. Lett.*, *42*(24), 10,704–10,713.
532 doi: 10.1002/2015GL065364
533 Zhang, R. (2015, April). Mechanisms for low-frequency variability of summer Arctic
534 sea ice extent. *Proc. Natl. Acad. Sci.*, *112*(15), 4570–4575. doi: 10.1073/pnas
535 .1422296112
536 Zheng, C., Ting, M., Wu, Y., Kurtz, N., Orbe, C., Alexander, P., ... Tedesco,
537 M. (2022, June). Turbulent Heat Flux, Downward Longwave Radiation,
538 and Large-Scale Atmospheric Circulation Associated with Wintertime Bar-
539 ents–Kara Sea Extreme Sea Ice Loss Events. *J. Climate*, *35*(12), 3747–3765.
540 doi: 10.1175/JCLI-D-21-0387.1
541 Zuo, H., Balmaseda, M. A., Tietsche, S., Mogensen, K., & Mayer, M. (2019, June).
542 The ECMWF operational ensemble reanalysis–analysis system for ocean and
543 sea ice: A description of the system and assessment. *J. Climate*, *15*(3), 779–
544 808. doi: 10.5194/os-15-779-2019